European Journal of Neuroscience, Vol. 11, pp. 2175–2181, 1999

SHORT COMMUNICATION
Can $GABA_A$ conductances explain the fast oscillation frequency of absence seizures in rodents?

Alain Destexhe
Départment de Physiologie, Université Laval, Québec G1K 7P4, Canada

Keywords: computational models, cortex, epilepsy, $GABA_B$, thalamus

Abstract

Rodent models of absence epilepsy generate spike-and-wave oscillations at relatively fast frequency (5–10 Hz) compared with humans (≈ 3 Hz). Possible mechanisms for these oscillations were investigated by computational models that included the complex intrinsic firing properties of thalamic and cortical neurons, as well as the multiple types of synaptic receptors mediating their interactions. The model indicates that oscillations with spike-and-wave field potentials can be generated by thalamocortical circuits. The frequency of these oscillations critically depended on GABAergic conductances in thalamic relay cells, ranging from 2–4 Hz for strong $GABA_B$ conductances to 5–10 Hz when $GABA_A$ conductances were dominant. This model therefore suggests that thalamocortical circuits can generate two types of spike-and-wave oscillations, whose frequency is determined by the receptor type mediating inhibition in thalamic relay cells. Experiments are proposed to test this mechanism.

Introduction

Absence epileptic seizures are associated with generalized spike-and-wave (SW) oscillations in the electroencephalogram. In human absence seizures, SW complexes typically recur at a slow frequency of ≈ 3 Hz (Porter, 1993). SW patterns are also seen in various animal models, including monkeys (Steriade, 1974), cats (Gloor & Fariello, 1988) and rodents (Marescaux *et al*., 1992). In cats and monkeys, the SW complexes are usually at a similar frequency (≈ 3 Hz) to that in human absences. However, in rodents, SW occurs at a faster frequency (5–10 Hz). The reasons for these frequency differences are presently unknown.

In the cat penicillin model of generalized epilepsy, absence seizures seem to depend on both thalamus and cortex, because they disappear if either of these structures are lesioned or inactivated (Pellegrini *et al*., 1979; Avoli & Gloor, 1981). Similar conclusions were also reached for the seizures of the generalized absence epilepsy rat from Strasbourg (GAERS) (Vergnes & Marescaux, 1992). In these experimental models, a critical role for the rebound burst mechanisms of thalamic neurons and of γ-aminobutyric acid (GABA) synaptic conductances of both $GABA_A$ and $GABA_B$ types was demonstrated (Vergnes *et al*., 1984; Gloor & Fariello, 1988; Liu *et al*., 1991, 1992; Hosford *et al*., 1992, 1997; Snead, 1992). The cellular mechanisms of SW therefore involve the complex intrinsic firing properties of thalamic and cortical neurons, interacting through multiple types of synaptic receptors, but due to the complexity of these interactions, the exact mechanisms remain unclear.

A recent computational model investigated a possible mechanism for SW which depended on mutual recruitment loops between cortical and thalamic cells (Destexhe, 1998). In this model, the burst responses of thalamic neurons and the particular properties of $GABA_B$ receptors were critical in generating oscillations with SW field potentials. In particular, the ≈ 3-Hz frequency was determined by $GABA_B$-mediated IPSPs in thalamocortical relay neurons, in agreement with observations in thalamic slices (von Krosigk *et al*., 1993). In contrast, $GABA_A$-mediated IPSPs have been found to pace TC cells during seizures characterized by fast-frequency SW (Pinault *et al*., 1998). In the present paper, computational models were used to investigate whether fast (5–10 Hz) and slow (2–3 Hz) SW oscillations can be generated by similar thalamocortical mechanisms.

Materials and methods

A thalamocortical network consisting of different one-dimensional layers of cortical and thalamic cells was simulated (Fig. 1, A1). The network included 100 thalamocortical relay cells (TC), 100 thalamic reticular (RE) neurons, 100 cortical pyramidal (PY) cells and 100 cortical interneurons (IN). The thalamus was thus represented by two homogeneous population of cells, with no interneurons, similar to most dorsal thalamic nuclei in rodents (Jones, 1985). The cortex was represented by a simplified representation of layer VI, in which PY cells constitute the major source of corticothalamic fibers. As corticothalamic cells receive a significant proportion of their excitatory synapses directly from ascending thalamic axons (Hersch & White, 1981; White & Hersch, 1982), these cells mediate a monosynaptic excitatory feedback loop (thalamus–cortex–thalamus), which was modelled here. Intrathalamic and intracortical connections were local and topographically organized, with each neuron contacting all other neurons within a radius of 5–10 cells (see details in Destexhe *et al*., 1998a).

Each cell type contained the minimal set of calcium- and voltage-dependent currents necessary to account for their intrinsic properties.

Correspondence: Dr A. Destexhe, Départment de Physiologie, Université Laval, Pavillon F. Vandry, Québec G1K 7P4, Canada.
E-mail: alain@fmed.ulaval.ca

Received 15 December 1998, revised 6 March 1999, accepted 9 March 1999

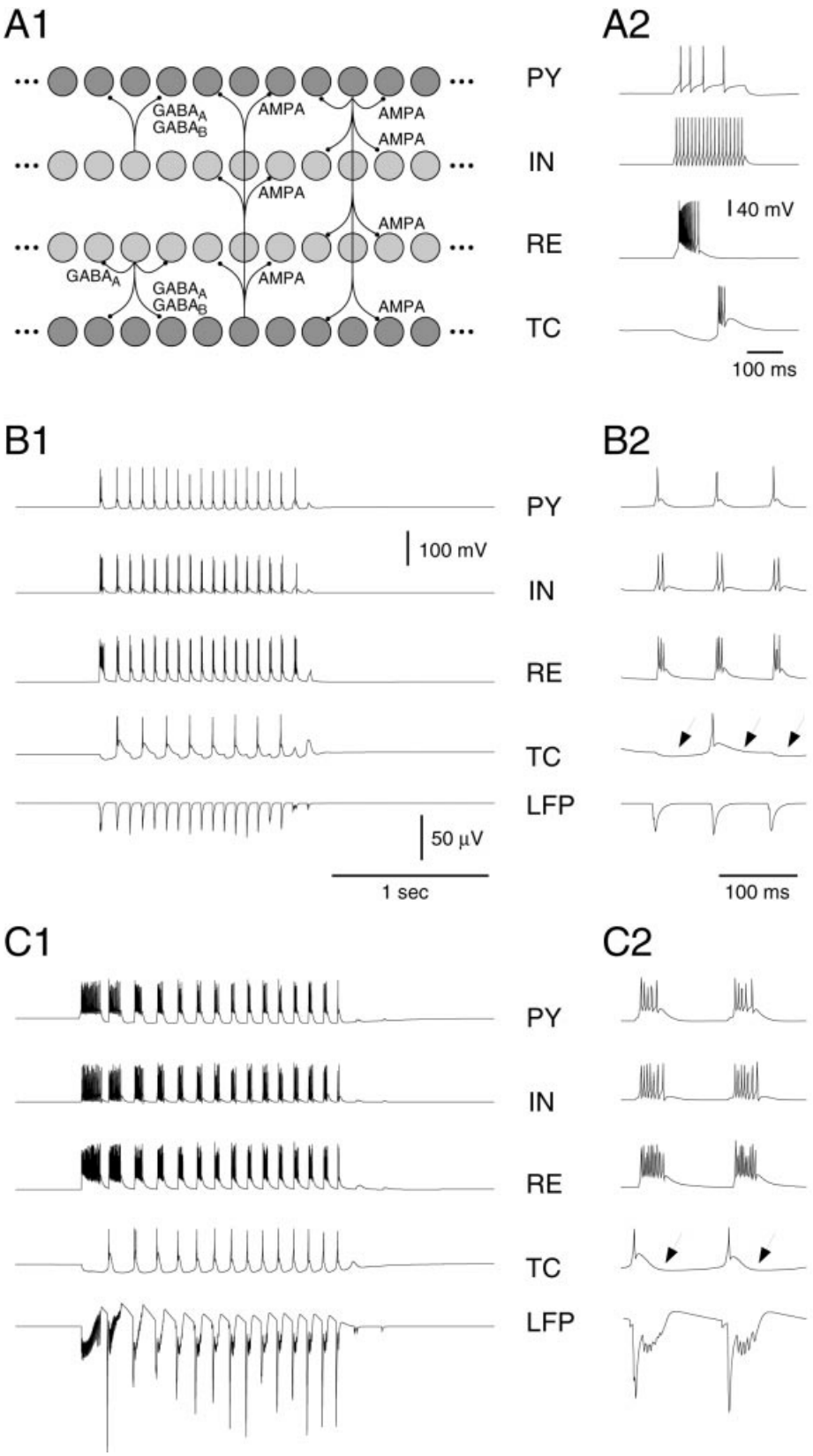
A1
A2
PY
IN
RE
TC
GABA$_A$
GABA$_B$
AMPA
40 mV
100 ms
B1
B2
100 mV
LFP
50 μV
1 sec
100 ms
C1
C2

All cells were single-compartment models containing the I_{Na} and I_{Kd} currents necessary to generate action potentials. In addition, TC cells had the low-threshold Ca^{2+} current I_T, a hyperpolarization-activated current I_h and a calcium-dependent upregulation of I_h; RE cells contained I_T; PY cells had a slow voltage-dependent K^+ current I_M responsible for spike-frequency adaptation, similar to 'regular-spiking' pyramidal cells (Connors & Gutnick, 1990). All currents were modelled using Hodgkin & Huxley (1952) type kinetics based on voltage-clamp data available for each cell type, as detailed previously (Destexhe *et al*., 1993; 1998a). The intrinsic firing properties of the different cell types are illustrated in Fig. 1 (A2).

Synaptic interactions were mediated by glutamate α-amino-3-hydroxy-5-methyl-4-isoxazolepropionic acid (AMPA) receptors, as well as GABAergic $GABA_A$ and $GABA_B$ receptors. These receptor types were simulated using kinetic models of postsynaptic receptors (Destexhe *et al*., 1998b): the decay time constants were of ≈ 5.5, 6.3 and 300 ms for AMPA-, $GABA_A$- and $GABA_B$-mediated currents, respectively. All excitatory connections (TC→RE, TC→IN, TC→PY, PY→PY, PY→IN, PY→RE and PY→TC) were mediated by AMPA receptors, some inhibitory connections (RE→TC, IN→PY) were mediated by a mixture of $GABA_A$ and $GABA_B$ receptors, while intra-RE connections were mediated by $GABA_A$ receptors (see scheme in Fig. 1, A1). Simulations were also performed using *N*-methyl-D-aspartate (NMDA) receptors added to all excitatory connections (with maximal conductance set to 25% of that of AMPA), but no appreciable difference was observed; they were therefore not included in the present figures.

Extracellular field potentials were calculated from PY cells using a model inspired by Nunez (1981). All cells were assumed to be arranged equidistantly in a one-dimensional layer with intercellular distances of 20 μm and the extracellular potential was calculated from postsynaptic currents and I_M (fast currents I_{Na} and I_{Kd} have a minimal contribution to distant field potentials and were excluded). The procedures for calculating field potentials were detailed in a previous paper (Destexhe, 1998).

The precise values of the parameters used here were identical to those used in a previous model (Destexhe, 1998), with three exceptions: (i) the leak reversal potential was adjusted in TC cells such that they had a resting membrane potential of –56 mV, as observed experimentally in the GAERS model (Pinault *et al*., 1998); (ii) the $GABA_B$ conductance from RE to TC was smaller than in the previous model (0.015 vs. 0.04 μS); and (iii) the $GABA_A$ conductance from RE to TC was larger than in the previous model (0.03 vs. 0.02 μS). The behaviour shown here was robust to changes in the parameters, such as the values of maximal conductance, the connectivity and the kinetics of currents. The robustness of the model was similar to the analysis done previously (see Destexhe, 1998).

All models of ion channels, single cells, networks and field potentials were simulated using the NEURON simulator (Hines & Carnevale, 1997) and were run on a Sparc 20 workstation (Sun Microsystems, Mountainview, CA, USA).

Results

The hypothesis investigated here was that slow (≈ 3 Hz) and fast (5–10 Hz) types of spike-and-wave seizures can be explained by the same thalamocortical mechanism, but they differ in the GABAergic receptor type ($GABA_A$ vs. $GABA_B$) governing inhibition in the thalamic TC cells. This hypothesis was investigated by simulating a thalamocortical network model (see Material and methods). In 'control' conditions, the network generated 8–12-Hz spindle oscillations, in which all cell types produced moderate rates of discharge approximately in phase, while the field potentials displayed successive negative deflections (Fig. 1B). Oscillations showed waxing-and-waning patterns, consisting of oscillatory sequences of 1–3 s recurring regularly at intervals of 10–20 s. The waxing-and-waning was due to upregulation of I_h by intracellular Ca^{2+} in TC cells (see details in Destexhe *et al*., 1998a). These features are in agreement with experimental observations in thalamic and cortical neurons during sleep spindles (Steriade *et al*., 1990). Spindle oscillations were not critically dependent on the strength of $GABA_A$ and $GABA_B$ conductances in TC cells (Destexhe *et al*., 1998a).

To obtain SW, the excitability of the network was enhanced through decreasing the effectiveness of $GABA_A$-mediated intracortical inhibition, similar to experiments with cortical application of penicillin (Gloor *et al*., 1977). In this case, the network generated a different type of oscillation (Fig. 1C). Cortical (PY and IN) and thalamic (RE) cells fired prolonged discharge patterns in synchrony, interleaved with periods of silence simultaneous in all cell types. This cellular pattern generated SW field potentials; the 'spike' component was generated by fast EPSPs shortly followed by $GABA_A$-mediated IPSPs in PY cells, while the positive 'wave' was due to activation of slow K^+ currents ($GABA_B$-mediated and voltage-dependent I_M) in PY cells.

Similar to a previous model of SW (Destexhe, 1998), this oscillatory pattern of discharge was produced by mutual recruitment loops between cortex and thalamus. Consequently, all conductances involved in the thalamocorticoreticular loop (TC→PY, PY→RE, RE→TC) were important. In addition, intracortical excitatory (PY→PY) connections played the central role of mediating the increase of cortical excitability leading to SW. In contrast, intrathalamic excitatory connections (TC→RE) had a minimal role, as suppressing them did not lead to appreciable changes in the SW oscillation (not shown). The latter connections were, however, necessary for spindling activity.

Unlike the previous model, the oscillation frequency was relatively fast in the present case (6–10 vs. 2–4 Hz). The fast frequency was due to the fact that the discharge of TC cells was shaped by $GABA_A$-mediated IPSPs (arrows in Fig. 1, C2). $GABA_B$ receptors also

FIG. 1. Thalamocortical loop model for fast spike-and-wave. (A) Scheme of the network and intrinsic neuronal properties. Cortical pyramidal (PY) neurons, cortical interneurons (IN), thalamic reticular (RE) neurons and thalamocortical (TC) neurons are shown with their interconnection pattern through AMPA, $GABA_A$ and $GABA_B$ receptors types (*left panel*). The intrinsic firing properties of these neurons (*right panel*) were simulated by Hodgkin–Huxley type of models for voltage-dependent currents (injected current was 0.75 nA for 200 ms for PY and IN, 0.3 nA for 10 ms for RE and –0.15 nA for 100 ms for TC). (B) Control spindle oscillations elicited by injection of a depolarizing current pulse in PY cells (1 nA for 20 ms). All cell types displayed moderate discharges at 10–12 Hz and the field potentials (LFP) consisted of negative deflections. Oscillations stopped due to upregulation of I_h by intracellular Ca^{2+} in TC cells. (C) Spike-and-wave oscillations following increase of cortical excitability (same simulation as in B, with intracortical $GABA_A$ conductances decreased from 0.15 to 0.04 μS). All cell types displayed synchronized discharges at 6–10 Hz and the field potentials consisted of spike-and-wave patterns. For B and C, the right panels show two oscillation cycles at higher temporal resolution. Arrows indicate $GABA_A$ IPSPs in TC cells.

contributed to the oscillation but produced a sustained hyperpolarization in TC and PY cells (see below).

The relative contribution of $GABA_A$ and $GABA_B$ conductances to the oscillation was investigated in TC cells. The time course of GABAergic conductances during SW (Fig. 2A) shows that $GABA_B$ conductances are tonically activated due to their slow kinetics, generating a sustained hyperpolarization in TC cells. This sustained hyperpolarization helped in maintaining oscillations, as diminishing $GABA_B$ conductances led to a markedly reduced tendency to oscillate (Fig. 2B, top trace), and increasing them led to a slow SW oscillation of a frequency of 2–3 Hz (Fig. 2B, bottom trace). This behaviour occurred for the whole parameter range for which the fast SW was present. The effect of a complete suppression of $GABA_B$ conductances depended on the strength of $GABA_A$ IPSPs; for weak $GABA_A$ conductances ($< 0.028\,\mu S$), blocking $GABA_B$ suppressed oscillations (Fig. 2C, top trace), whereas for stronger $GABA_A$ conductances ($> 0.028\,\mu S$), blocking $GABA_B$ reduced the number of cycles and increased the frequency (Fig. 2C, bottom trace).

Fast SW oscillations were also sensitive to alterations of $GABA_A$ conductances in TC cells. Reducing the conductance of $GABA_A$ IPSPs markedly reduced oscillatory sequences (Fig. 2D, top trace) while increasing them led to prolonged oscillations (Fig. 2D, bottom trace). This effect was seen for all parameters tested. Suppressing $GABA_A$ conductances in TC cells had two possible effects depending on the value of $GABA_B$ conductances; for strong $GABA_B$ conductances ($> 0.01\,\mu S$), blocking $GABA_A$ shortened the oscillatory sequence (Fig. 2E, top trace), but if $GABA_B$ conductances were too small ($< 0.01\,\mu S$), blocking $GABA_A$ suppressed oscillatory behaviour (Fig. 2E, bottom trace). Finally, when $GABA_A$ conductances were suppressed in both TC and RE cells, the system switched from fast SW to slow SW of ≈ 3–4 Hz (Fig. 2F). Here again, this behaviour was seen only if $GABA_B$ conductances were strong enough ($> 0.01\,\mu S$).

These properties were summarized by surface plots showing how $GABA_A$ and $GABA_B$ conductances determine the oscillation frequency (Fig. 3A) and duration (Fig. 3B). These plots show that (i) no SW oscillation arose if both GABAergic conductances were too low ($< 0.01\,\mu S$); (ii) only slow (≈ 3 Hz) SW oscillations were seen for large $GABA_B$ and low $GABA_A$ conductances; (iii) only fast (≈ 10 Hz) SW oscillations were seen for small $GABA_B$ and large $GABA_A$ conductances; and (iv) for intermediate values, the transition between fast and slow SW was relatively smooth (Fig. 3A). Note that fast SW oscillations may occur at a frequency similar to spindles (7–14 Hz) but in fact constitute a distinct oscillation type (see Fig. 1B–C).

The above observations suggest that fast and slow SW oscillations are part of a continuum of oscillatory states, in which frequency and duration are determined by the relative values of $GABA_A$ and $GABA_B$ conductances in TC cells. Thus, it should be possible to alter the frequency of SW oscillations by manipulating GABAergic conductances. These experimentally testable predictions of the model are discussed below.

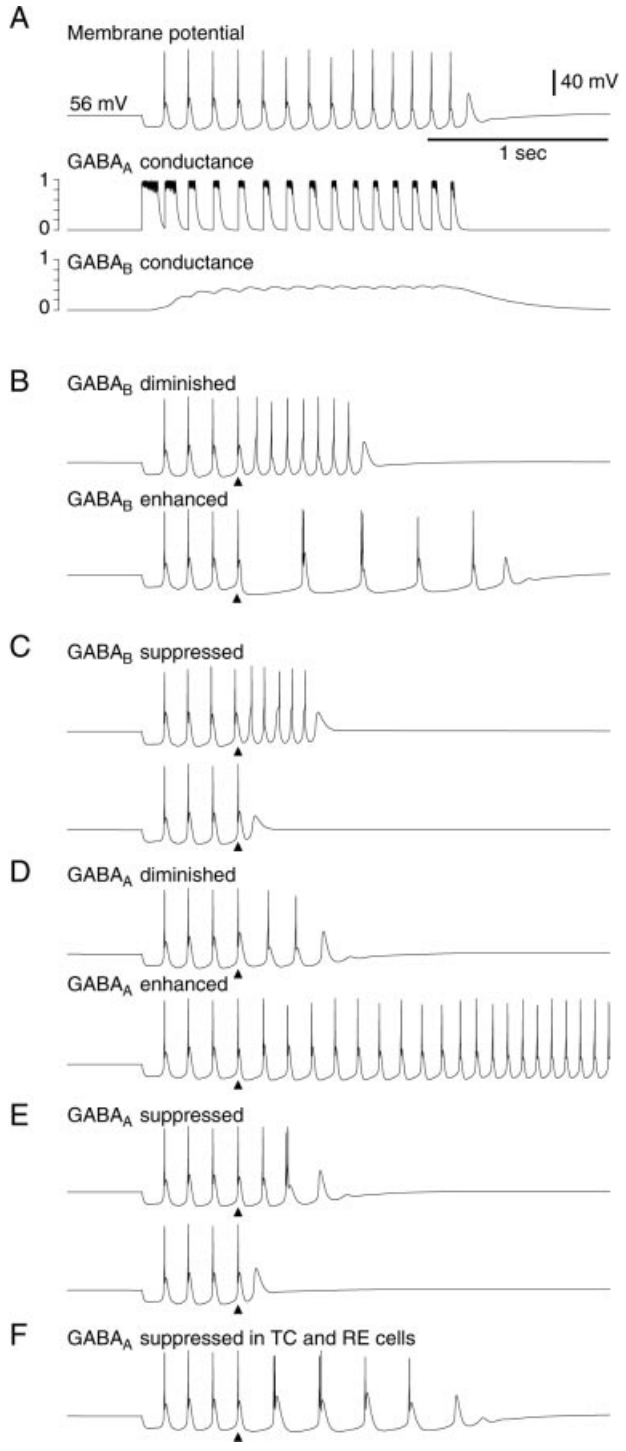

FIG. 2. Properties of fast spike-and-wave. All traces show manipulations of TC cells in a simulation similar to that of Fig. 1C. (A) Time course of GABAergic conductances in TC cells: membrane potential of a representative TC cell (*top trace*); fraction of $GABA_A$ conductance activated (*middle trace*); and fraction of $GABA_B$ conductance activated (*bottom trace*). Same simulation as in Fig. 1C (maximal conductances were $g_{GABAA} = 0.03\,\mu S$ and $g_{GABAB} = 0.015\,\mu S$). (B) $GABA_B$ receptors prolong oscillatory activity. Diminishing $GABA_B$ conductances (arrow) in all TC cells (*top trace*; $g_{GABAB} = 0.005\,\mu S$) shortened oscillations while stronger $GABA_B$ conductances had the opposite effect (*bottom trace*; $g_{GABAB} = 0.04\,\mu S$). (C) Blocking $GABA_B$ conductances (arrow) resulted in either shortening (*top trace*; $g_{GABAA} = 0.04\,\mu S$) or suppression of oscillatory behaviour (*bottom trace*; $g_{GABAA} = 0.02\,\mu S$). (D) $GABA_A$ conductances exacerbate oscillatory behaviour. Diminishing $GABA_A$ conductances (arrow) in TC cells (*middle trace*; $g_{GABAA} = 0.01\,\mu S$) shortened oscillations while augmenting them led to sustained oscillations (*bottom trace*; $g_{GABAA} = 0.06\,\mu S$). (E) Blocking $GABA_A$ conductances (arrow) in TC cells either shortened the oscillatory sequence (top trace; $g_{GABAB} = 0.015\,\mu S$) or suppressed oscillatory behaviour (*bottom trace*; $g_{GABAB} = 0.005\,\mu S$). (F) Suppressing $GABA_A$ conductances in both TC and RE cells (arrow) switched the system to slow SW at 3–4 Hz.

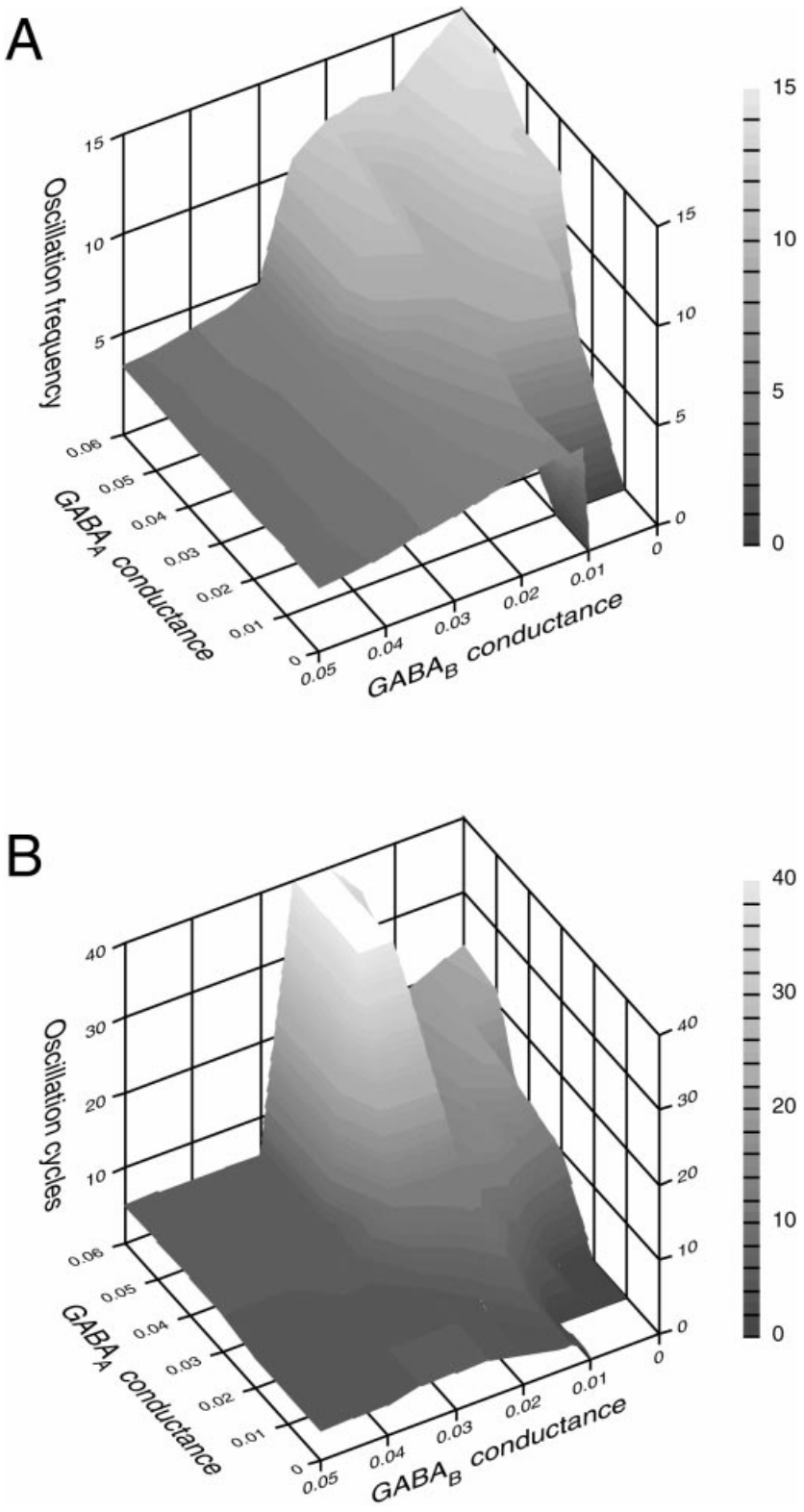

FIG. 3. Dependence of spike-and-wave oscillation frequency and duration on GABAergic conductances. The oscillation frequency and number of cycles were determined from the time of the first action potential in TC cells in simulations similar to that in Fig. 1C. (A) Two-dimensional representation of the frequency of SW oscillations as a function of $GABA_A$ and $GABA_B$ conductances in TC cells (in μS). The frequency was displayed using a grey scale ranging from 0 Hz (no oscillation; dark grey) to 15 Hz (light grey; see grayscale bar). (B) Same representation for the number of oscillation cycles, which were represented using a grey scale ranging from 0 (no oscillation; dark grey) to 40 cycles (light grey; see scale bar). The highest peak corresponds to sustained oscillations and was truncated at 40 cycles.

Discussion

The mechanism of fast spike-and-wave oscillations analysed in this paper displays striking similarities with rodent models of generalized absence epilepsy. A number of intracellular observations in the GAERS model (Charpier *et al*., 1998; Pinault *et al*., 1998) are present in this model (Fig. 1C): (i) the relatively depolarized resting level of TC cells (≈ –56 mV); (ii) the relatively moderate discharge of TC cells during the 'spike' component of SW; (iii) the presence of $GABA_A$ IPSPs in TC cells during the 'wave' component; (iv) the presence of a sustained hyperpolarization in TC and PY cells, which was due here to tonic activation of $GABA_B$ receptors (Fig. 2A); and (v) the presence of an afterdepolarization in TC cells following the seizure, which was due here to upregulation of I_h (not shown here, but see Destexhe, 1998). In addition, the model is consistent with several general properties of rodent SW: (i) all cell types discharge during the 'spike' (with TC cells firing slightly earlier), while the 'wave' coincides with neuronal silence (Buzsaki *et al*., 1988; Inoue *et al*., 1993; Seidenbecher *et al*., 1998; see Fig. 1, C2); (ii) antagonizing $GABA_B$ receptors in TC cells antagonizes SW (Liu *et al*., 1992; see Fig. 2B–C); (iii) enhancing $GABA_A$ receptors exacerbates SW (Vergnes *et al*., 1984; Hosford *et al*., 1997; see Fig. 2D); and (iv) the oscillation is generated by thalamocortical loops, which agrees with the observation that the integrity of both cortex and thalamus is necessary for generating seizures in the GAERS model (Vergnes & Marescaux, 1992).

The nature of the firing of TC cells during absence seizures has been recently debated. Some experiments reported burst firing of TC cells (McCormick & Hashemiyoon, 1998; Seidenbecher *et al*., 1998) in contrast to others (Steriade & Contreras, 1995; Pinault *et al*., 1998). In the model, TC cells fired low-threshold spike bursts in rebound to $GABA_A$ IPSPs. However, these bursts were weak and often consisted of single spikes (Fig. 1, C2). This was due to the relatively depolarized level of TC cells (–56 mV) at which $GABA_A$ IPSPs could only partially deinactivate the T-current. Such 'weak' rebound bursts may therefore be difficult to identify, which may explain the contrasting experimental observations outlined above. Rebound bursts also play a central role in the oscillatory mechanism because they trigger the spike–wave discharge in the entire network (Fig. 1, C2), in agreement with the experimental observation that TC cells discharge in advance of other cell types (Inoue *et al*., 1993; Pinault *et al*., 1998; Seidenbecher *et al*., 1998).

The similarity of this mechanism with that proposed for 3-Hz SW (Destexhe, 1998) suggests that fast and slow types of SW may be generated by similar thalamocortical recruitment mechanisms based on IPSP-rebound sequences in TC cells, and that the frequency therefore depends on the receptor type ($GABA_A$ vs. $GABA_B$) mediating these IPSPs. The model generates a series of predictions to test this mechanism in rodents: (i) blocking the T-current in TC cells should suppress seizures; (ii) reinforcing $GABA_B$ conductances in TC cells should slow down the frequency of SW to ≈ 3 Hz (Fig. 2B); (iii) blocking $GABA_B$ receptors in TC cells should reduce or suppress seizures (Fig. 2C); and (iv) suppressing thalamic $GABA_A$ conductances should lead to either complete suppression of seizures or should transform fast SW into slow SW (Fig. 2E–F). The model therefore suggests several experiments to transform the fast SW of rodents into ≈ 3 Hz SW by manipulating GABAergic receptors in the thalamus, but the success of these experiments relies on the condition that $GABA_B$ conductances are strong enough to sustain slow SW (see Fig. 3A). The opposite transformation, from ≈ 3 Hz SW to fast SW, should also be possible by antagonizing $GABA_B$ receptors and/or by reinforcing $GABA_A$ conductances in TC cells. If these predictions can be verified experimentally, then the present model suggests that different experimental models of absence epilepsy may correspond to the same cellular mechanisms even though they display very different frequencies.

Acknowledgements

Research supported by the Medical Research Council of Canada (MT-13724).

Abbreviations

AMPA, α-amino-3-hydroxy-5-methyl-4-isoxazolepropionic acid; EPSP, excitatory postsynaptic potential; GABA, γ-aminobutyric acid; GAERS, generalized absence epilepsy rat from Strasbourg; IN, cortical interneuron; IPSP, inhibitory postsynaptic potential; PY, cortical pyramidal; RE, thalamic reticular; SW, spike-and-wave; TC, thalamocortical.

References

Avoli, M. & Gloor, P. (1981) The effect of transient functional depression of the thalamus on spindles and bilateral synchronous epileptic discharges of feline generalized penicillin epilepsy. *Epilepsia*, **22**, 443–452.

Buzsaki, G., Bickford, R.G., Ponomareff, G., Thal, L.J., Mandel, R. & Gage, F.H. (1988) Nucleus basalis and thalamic control of neocortical activity in the freely moving rat. *J. Neurosci.*, **8**, 4007–4026.

Charpier, S., Deniau, J.M., Mahon, S., Leresche, N., Hughes, S.W. & Crunelli, V. (1998) *In vivo* intracellular recordings in cortical neurons during spontaneous spike and wave discharges in a genetic model of absence epilepsy. *Soc. Neurosci. Abstr.*, **24**, 1210.

Connors, B.W. & Gutnick, M.J. (1990) Intrinsic firing patterns of diverse neocortical neurons. *Trends Neurosci.*, **13**, 99–104.

Destexhe, A. (1998) Spike-and-wave oscillations based on the properties of $GABA_B$ receptors. *J. Neurosci.*, **18**, 9099–9111.

Destexhe, A., Contreras, D. & Steriade, M. (1998a) Mechanisms underlying the synchronizing action of corticothalamic feedback through inhibition of thalamic relay cells. *J. Neurophysiol.*, **79**, 999–1016.

Destexhe, A., Mainen, Z.F. & Sejnowski, T.J. (1998b) Kinetic models of synaptic transmission. In Koch, C. & Segev, I. (eds), *Methods in Neuronal Modeling,* 2nd edn. MIT Press, Cambridge MA, pp. 1–26.

Destexhe, A., McCormick, D.A. & Sejnowski, T.J. (1993) A model for 8–10 Hz spindling in interconnected thalamic relay and reticularis neurons. *Biophys. J.*, **65**, 2474–2478.

Gloor, P. & Fariello, R.G. (1988) Generalized epilepsy: some of its cellular mechanisms differ from those of focal epilepsy. *Trends Neurosci.*, **11**, 63–68.

Gloor, P., Quesney, L.F. & Zumstein, H. (1977) Pathophysiology of generalized penicillin epilepsy in the cat: the role of cortical and subcortical structures. II. Topical application of penicillin to the cerebral cortex and subcortical structures. *Electroencephalogr. Clin. Neurophysiol.*, **43**, 79–94.

Hersch, S.M. & White, E.L. (1981) Thalamocortical synapses on corticothalamic projections neurons in mouse SmI cortex: electron microscopic demonstration of a monosynaptic feedback loop. *Neurosci. Lett.*, **24**, 207–210.

Hines, M.L. & Carnevale, N.T. (1997) The NEURON simulation environment. *Neural Comput.*, **9**, 1179–1209.

Hodgkin, A.L. & Huxley, A.F. (1952) A quantitative description of membrane current and its application to conduction and excitation in nerve. *J. Physiol. (Lond.)*, **117**, 500–544.

Hosford, D.A., Clark, S., Cao, Z., Wilson, W.A. Jr, Lin, F.H., Morrisett, R.A. & Huin, A. (1992) The role of $GABA_B$ receptor activation in absence seizures of lethargic (lh/lh) mice. *Science*, **257**, 398–401.

Hosford, D.A., Wang, Y. & Cao, Z. (1997) Differential effects mediated by $GABA_A$ receptors in thalamic nuclei of lh/lh model of absence seizures. *Epilepsy Res.*, **27**, 55–65.

Inoue, M., Duysens, J., Vossen, J.M.H. & Coenen, A.M.L. (1993) Thalamic multiple-unit activity underlying spike-wave discharges in anesthetized rats. *Brain Res.*, **612**, 35–40.

Jones, E.G. (1985) *The Thalamus,* Plenum Press, New York.

von Krosigk, M., Bal, T. & McCormick, D.A. (1993) Cellular mechanisms of a synchronized oscillation in the thalamus. *Science*, **261**, 361–364.

Liu, Z., Vergnes, M., Depaulis, A. & Marescaux, C. (1991) Evidence for a

critical role of GABAergic transmission within the thalamus in the genesis and control of absence seizures in the rat. *Brain Res.*, **545**, 1–7.
Liu, Z., Vergnes, M., Depaulis, A. & Marescaux, C. (1992) Involvement of intrathalamic $GABA_B$ neurotransmission in the control of absence seizures in the rat. *Neuroscience*, **48**, 87–93.
Marescaux, C., Vergnes, M. & Depaulis, A. (1992) Genetic absence epilepsy in rats from Strasbourg – a review. *J. Neural Transmission*, **35** (Suppl.), 37–69.
McCormick, D.A. & Hashemiyoon, R. (1998) Thalamocortical neurons actively participate in the generation of spike-and-wave seizures in rodents. *Soc. Neurosci. Abstr.*, **24**, 129.
Nunez, P.L. (1981) Electric Fields of the Brain. *The Neurophysics of EEG,* Oxford University Press, Oxford.
Pellegrini, A., Musgrave, J. & Gloor, P. (1979) Role of afferent input of subcortical origin in the genesis of bilaterally synchronous epileptic discharges of feline generalized epilepsy. *Exp. Neurol.*, **64**, 155–173.
Pinault, D., Leresche, N., Charpier, S., Deniau, J.M., Marescaux, C., Vergnes, M. & Crunelli, V. (1998) Intracellular recordings in thalamic neurones during spontaneous spike and wave discharges in rats with absence epilepsy. *J. Physiol. (Lond.)*, **509**, 449–456.
Porter, R.J. (1993) The absence epilepsies. *Epilepsia*, **34** (Suppl.), S42–S48.
Seidenbecher, T., Staak, R. & Pape, H.C. (1998) Relations between cortical and thalamic cellular activities during absence seizures in rats. *Eur. J. Neurosci.*, **10**, 1103–1112.
Snead, O.C. (1992) Evidence for $GABA_B$-mediated mechanisms in experimental generalized absence seizures. *Eur. J. Pharmacol.*, **213**, 343–349.
Steriade, M. (1974) Interneuronal epileptic discharges related to spike-and-wave cortical seizures in behaving monkeys. *Electroencephalogr. Clin. Neurophysiol.*, **37**, 247–263.
Steriade, M. & Contreras, D. (1995) Relations between cortical and thalamic cellular events during transition from sleep patterns to paroxysmal activity. *J. Neurosci.*, **15**, 623–642.
Steriade, M., Jones, E.G. & Llinas, R.R. (1990) *Thalamic Oscillations and Signalling,* John Wiley Sons, New York.
Vergnes, M. & Marescaux, C. (1992) Cortical and thalamic lesions in rats with genetic absence epilepsy. *J. Neural Transmission*, **35** (Suppl.), 71–83.
Vergnes, M., Marescaux, C., Micheletti, G., Depaulis, A., Rumbach, L. & Warter, J.M. (1984) Enhancement of spike and wave discharges by GABAmimetic drugs in rats with spontaneous petit-mal-like epilepsy. *Neurosci. Lett.*, **44**, 91–94.
White, E.L. & Hersch, S.M. (1982) A quantitative study of thalamocortical and other synapses involving the apical dendrites of corticothalamic cells in mouse SmI cortex. *J. Neurocytol.*, **11**, 137–157.